dition at the interface. This subject will be discussed in a further report.

P. K. Currie has obtained independently similar theoretical results. A detailed numerical calculation together with a comparison with Currie's description will be given elsewhere.

*Laboratoire associé au Centre National de la Recherche Scientifique.

[1]E. Dubois-Violette, C. R. Acad. Sci. 21, 275, 923 (1971).

[2]E. F. Carr, Mol. Cryst. Liquid Cryst. 7, 253 (1969).

[3]W. Helfrich, J. Chem. Phys. 51, 4092 (1969).

[4]E. Dubois-Violette, E. Guyon, and P. Pieranski, in Proceedings of the International Conference on Liquid Crystals, Kent, Ohio, 1972 (Mol. Cryst. Liquid Cryst., to be published).

[5]P. Pieranski, F. Brochard, and E. Guyon, J. Phys. (Paris) 33, 681 (1972).

[6]I. Haller, J. Chem. Phys. 57, 1400 (1972).

[7]A more complete discussion of the "stabilizing" or "destabilizing" character of this dissipative torque can be found in Ref. 3 and in F. M. Leslie, Quart. J. Mech. Appl. Math. 19, 357 (1966); O. Parodi, J. Phys. (Paris) 31, 581 (1970).

[8]Of course, for samples with $\kappa_a = 0$, the usual Bénard process, for isotropic liquids heated from below, takes place. But as soon as $\kappa_a < 10^{-6}$ cm^2 sec^{-1} the anisotropic mechanism is the dominant one.

[9]We use the notations and values of the viscosity coefficients given by Ch. Gähwiller, Phys. Lett. 36A, 311 (1971).

[10]In isotropic liquids, the formation of hexagons is observed when the viscosity changes with temperature are important. A general discussion of heat-convection effects in isotropic liquids is given in S. Chandrasekhar, *Hydrodynamic and Hydromagnetic Stability* (Oxford Univ. Press, Oxford, England, 1961).

Nonlinear Behavior of Stimulated Brillouin and Raman Scattering in Laser-Irradiated Plasmas*

D. W. Forslund, J. M. Kindel, and E. L. Lindman
University of California, Los Alamos Scientific Laboratory, Los Alamos, New Mexico 87544
(Received 4 December 1972)

Both analytic theory and inhomogeneous plasma simulations are presented to show the nonlinear development of the Brillouin and Raman backscatter instabilities. Nonlinear fluid behavior predicts a backscatter energy on the order of the incident laser energy, but particle trapping and heating effects associated with the excited electrostatic wave can significantly reduce this.

When laser light above certain power levels irradiates a plasma, collective processes occur which can either enhance[1] or retard the light absorption.[2-5] In the latter case the incident energy is reflected by the plasma through the decay of the incident light wave into a backward-traveling light wave and either a low-frequency ion wave (stimulated Brillouin scattering) or an electron plasma wave (stimulated Raman scattering). The energy in the light wave is thus prevented from arriving at the critical surface (that place in the plasma were the plasma frequency equals the light-wave frequency) where enhanced absorption can take place. Since energy absorption[1] is crucial in laser fusion and ionospheric radar modification applications,[6] a knowledge of the penetration depth allowed by these instabilities and the incident energy reflected is required.

These backscatter instabilities[2] are examples of the backward wave oscillator problem. The temporal linear theory (real k, complex ω) and the spatial linear theory (complex k and ω) have appeared in the literature.[7]

Nonlinear problem.—As in the linear theory the fluid equations for ions and electrons are combined with Maxwell's equations using the vector potential formalism,[3b] but the reaction of the backscattered and electrostatic waves on the pump wave is no longer neglected. As discussed in Ref. 2, there are three linear waves excited by the circularly polarized pump wave, two electromagnetic and one electrostatic. In both the Brillouin and Raman problems, one of the electromagnetic waves, the forward scattered wave, is not in resonance and can be neglected. Insofar as electrostatic steepening terms and higher-order mode coupling terms are negligible, the following set of equations describe both the Brillou-

in and Raman instability evolution:

$$\left(\frac{\partial^2}{\partial t^2} - c^2\frac{\partial^2}{\partial x^2} + \omega_{pe}^2\right)\vec{A}_{-1} = -\omega_{pe}^2\frac{n_e}{n_0}\vec{A}_{i-1}, \quad i=0,1, \tag{1}$$

$$\frac{\partial^2 n_e}{\partial t^2} + \gamma_d\frac{\partial n_e}{\partial t} - \gamma v_e^2\frac{\partial^2 n_e}{\partial x^2} + \omega_{pe}^2(n_e - n_i) = \frac{e^2 n_0}{m_e^2 c^2}\frac{\partial^2}{\partial x^2}(\vec{A}_0\cdot\vec{A}_{-1}), \tag{2}$$

$$\frac{\partial^2 n_i}{\partial t^2} + \omega_{pi}^2(n_i - n_e) = 0. \tag{3}$$

In these equations, $\vec{A}_0$ or $\vec{A}_{-1}$ is the vector potential of the pump or backscattered wave, n_j is the density fluctuation, ω_{pj} is the plasma frequency of the jth species, $v_e^2 = T_e/m_e$, γ_d is the damping rate of the electrostatic wave, and γ is the ratio of the specific heats and is equal to 1 or 3. The ion temperature T_i is taken to be zero.

For the temporal problem, after Fourier analyzing in x, Eqs. (1)–(3) describe three coupled harmonic oscillators whose behavior in time is quite different depending on whether the linear growth rate Γ of the instability is large or small compared to the uncoupled frequency Ω of the electrostatic wave. Expressions for the growth rates[2-5] (for $\Gamma < \Omega$ and $\gamma_d = 0$) of these instabilities are $\Gamma = \omega_{pe}kv_0/|8\Omega\omega_{-1}M_i/m_e|^{1/2}$ for the Brillouin case, where $\Omega \equiv \omega_s \equiv kc_s$, $c_s = (\gamma T_e/M_i)^{1/2}$, and $\Gamma = \omega_{pe}kv_0/|8\Omega\omega_{-1}|^{1/2}$ for the Raman case, where $\Omega \equiv \omega_i \equiv (\omega_{pe}^2 + \gamma k^2 v_e^2)^{1/2}$. In the above expressions $v_0 = e|E_0|/m_e\omega_0$, $E_0 \equiv (\omega_0/c)A_0$, ω_0 and k_0 are the incident laser frequency and wave number, $\omega_{-1} = \Omega - \omega_0$, and $k \approx 2k_0$ is the wave number of the electrostatic wave.

In the weak coupling limit ($\Gamma < \Omega$), the solutions of similar equations which have been described elsewhere[8] show that A_{-1} or E_{-1} reaches its peak value of $E_{-1}^2/|\omega_{-1}| = E_0^2(0)/|\omega_0|$ at the same time that n_e/n_0 reaches its peak value. This behavior is modified by particle trapping if the electrostatic plasma wave becomes sufficiently large such that $v_{\text{trap}} \equiv (2eE/mk)^{1/2} > \Omega/k - 2v_{\text{th}}$,[1a] where E is the electric field of the electrostatic wave. This effect leads to an increase in the damping of the density fluctuation n_e and production of high-velocity particles in phase space (non-Maxwellian tail formation). And, of course, if n_e/n_0 exceeds unity at some point in the oscillation, wave breaking occurs and the oscillations predicted by the fluid equations cease.

In the strong coupling limit[2,3] ($\Gamma > \Omega$), the linear growth stage also stops when the backward-traveling light wave reaches nearly equal amplitude with the pump. The density continues to evolve, and in the Brillouin case is given approximately by

$$\frac{n_e}{n_0} \approx \frac{v_0^2}{v_e^2}\left\{1 - \cos[\omega_s(t - t_{\text{sat}})] + \frac{\omega_s^2}{\Gamma^2}\right\}. \tag{4}$$

To arrive at Eq. (4) from Eqs. (1)–(3), assume $\vec{A}_0\cdot\vec{A}_{-1}$ is time independent and let $n_e \cong n_i$ and $\gamma_d = 0$. Equation (2) can then be integrated. In the strong-coupling regime $\Gamma \sim (\omega_{pi}^2 k^2 v_0^2/\omega_0)^{1/3}$. If n_e/n_0 remains less than 1 and negligible particle trapping occurs ($v_{\text{trap}} < \Omega/k - 2v_{\text{th}}$), the system oscillates according to Eq. (4). If particle trapping occurs, the oscillations are damped. If $v_0/v_e > 1$, however, the wave breaks and the oscillations predicted by the fluid equations cease, as verified by simulations.[9]

In the weak-coupling limit and for $\gamma_d = 0$, the procedure used in Ref. 8 for the temporal problem can be applied to the spatial problem and analytic solutions can be obtained. If Eqs. (1)–(3) are Fourier analyzed in time, a standard analysis with small amplitude variations over a wavelength can be carried out.[10] Equations (1)–(3) reduce in steady state to

$$\frac{\partial\alpha_i}{\partial x} = \frac{\omega_{pe}^2}{c^2}\frac{\alpha_{i-1}}{k_{-i}}\frac{n_e}{n_0}, \quad i=0,1,$$
$$\omega\frac{\gamma_d}{2}\frac{n_e}{n_0} + kv^2\frac{\partial}{\partial x}\frac{n_e}{n_0} = -\frac{1}{2}k^2c^2\alpha_0\alpha_{-1}, \tag{5}$$

where $k_{-1} = k - k_0$, $\alpha_i = eA_i/(m_e M_i c^4)^{1/2}$, and $v = c_s$ for the Brillouin problem, and $\alpha_i = eA_i/(m_e c^2)$ and $v = \gamma^{1/2}v_e$ for the Raman problem. The temporal stability of the solutions of these equations for weak damping has not been examined.[11] For $\gamma_d = 0$, the solution to the infinite half-space problem is $\alpha_0 = (k_{-1}/k_0)^{1/2}\alpha_{-1} = \alpha_0(0)\,\text{sech}(x/L_1)$, where

$$L_1 = 4\gamma^{1/2}\frac{v_e}{v_0(0)}\left(\frac{k_{-1}}{k_0}\right)^{1/2}\frac{c}{\omega_{pe}} \sim 4\lambda_D\frac{c}{v_0}.$$

This solution corresponds to nearly total reflection with an evanescence length L_1. Computer simulation studies verify this small evanescence length only when the electrostatic wave remains

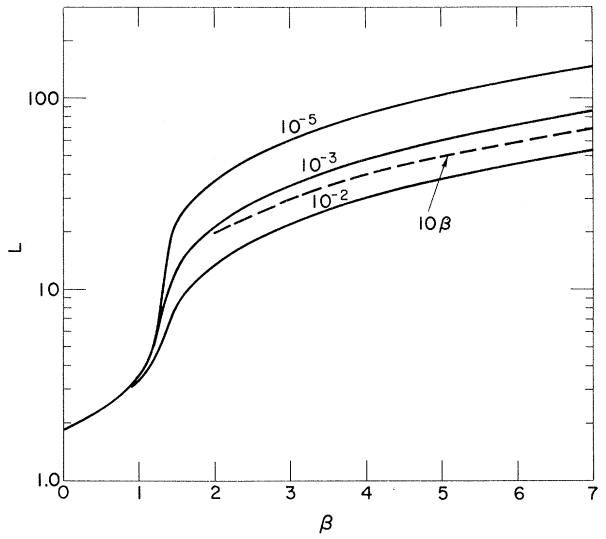

FIG. 1. Length of plasma, L, in units of L_1 as a function of β for 50% energy reflection for three values of ϵ. For comparison, $L=10\beta$ is plotted.

of sufficiently small amplitude to preclude nonlinear damping effects. If a density gradient is allowed, an additional wave-number mismatch term must be included in Eq. (5) which can further reduce the backscatter.

In order to obtain better agreement with the computer simulations, a finite γ_d must be allowed, implying that dissipation due to particle trapping is important. When the damping is sufficiently large such that $\beta \equiv \frac{1}{4}\gamma_d L_1 \omega/kv^2 \gg 1$, the problem formally reduces to stimulated Brillouin or Raman scattering in solids for which a nonlinear theory exists.[11] From Tang's theory,[11] the penetration depth of the incident laser is large, typically $L \sim 10\beta L_1$. For Brillouin scattering $\beta \sim k\lambda_D(\gamma_d/\omega_s)c/v_0$.

For arbitrary γ_d, Eq. (5) can be solved numerically to obtain the reflection from a plasma slab of thickness L with the boundary conditions $n_1(0) = 0$, $\alpha_0(0)$ and $\alpha_{-1}(L) = \epsilon$, where ϵ is the noise level. Figure 1 shows the thickness as a function of β for 50% reflection. In laser fusion applications it is desired, of course, that this length exceed the distance to the critical surface where strong absorption can take place.

Simulation studies of saturation.—A large number of one-dimensional simulations in homogeneous plasmas have been carried out in which careful choice of parameters has allowed isolation of the various types of behavior discussed above.[2] The results of these idealized cases support the above theoretical treatment, while the simulation of a more realistic problem in which both instabilities occur simultaneously is discussed below.

Figure 2 summarizes the results for this case

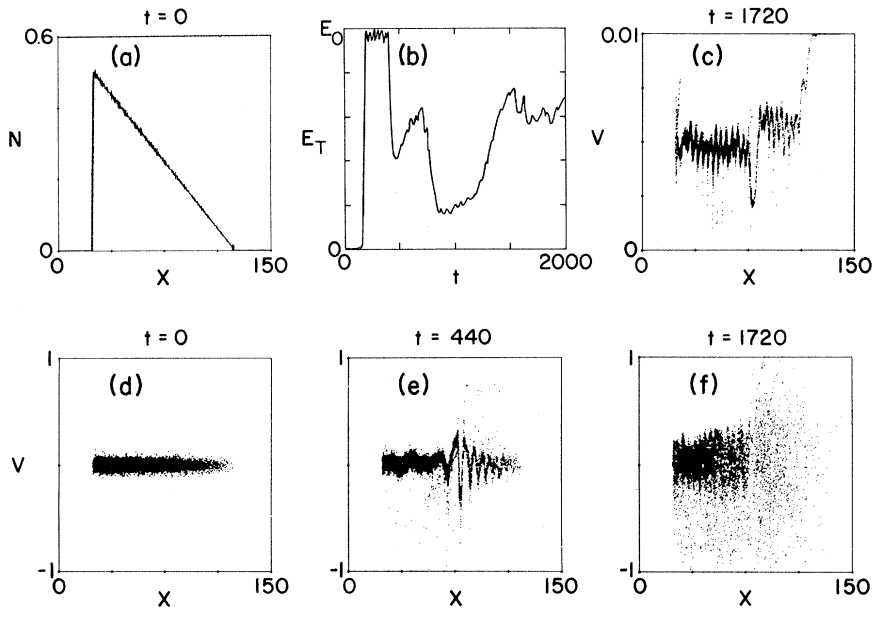

FIG. 2. (a) Density profile, and (c) ion and (d)–(f) electron X-V_X phase-space plots at noted times in units of ω_0^{-1} for a simulation with parameters $n_{max}/n_c = 0.5$, $v_0/c = 0.1$, $M_i/m_e = 1836$, $T_e/T_i = 10$, $v_e/c = 0.05$, a system length of $150c/\omega_0$, 20 000 simulation particles, 1024 cells, and time step $2\omega_0^{-1}$. V is the X velocity in units of c. (b) Transmitted electric field amplitude through the left boundary of density profile.

in which a laser light wave is launched from the right into the subcritical ($n_{max}/n_c \sim 0.5$, where $\omega_{pe} = \omega_0$ at n_c) plasma whose initial density profile is shown in Fig. 2(a). The transmitted light and the high-energy particle flux are monitored and absorbed at the left-hand boundary of the simulation plasma. Figure 2(b) shows the amplitude of the transmitted light at the left boundary as a function of time. Initially, there is 100% transmission. The first minimum occurs at $t = 500\omega_0^{-1}$ and is due to the Raman instablity. The second minimum, occuring around $t = 1000\omega_0^{-1}$, is due to the Brillouin instability. At the end of the run 40% transmission is obtained because the electron heating has increased L_1 and thus the penetration depth.

Figure 2(e) shows the excited electron plasma wave at $t = 440\omega_0^{-1}$ due to the Raman instability which is very coherent at this point and thus able to cause strong reflection; the initial electron phase space is shown in Fig. 2(d) for comparison. A similar behavior (not shown) is seen in the ion phase space at $t = 1000\omega_0^{-1}$. Figures 2(c) and 2(f) show ion and electron phase space at $t = 1720\omega_0^{-1}$. The ion wave in the Brillouin instability is clearly evident. The substantial electron heating from $t = 440\omega_0^{-1}$ to $t = 1720\omega_0^{-1}$ is due to strong electron trapping.

At $t = 1720\omega_0^{-1}$, the hot electron energy flux at the plasma boundary ($x = 25c/\omega_0$) is about 25% of the incident laser energy flux. Most of the electron heating results from the Raman instability which, from a simple energetics argument using the fluid equations, is capable of absorbing 50% of the incidnet laser energy at densities near $n/n_c = \frac{1}{4}$, the critical surface for the backward light wave. The electron heating, in fact, is causing the low-density ion blowoff seen in Fig. 2(c).

Application to experiments.—Inhomogeneous thresholds are usually more important than collisional thresholds in experiments. In an inhomogeneous plasma, the threshold condition for the Brillouin instability is $v_0^2/v_e^2 > 4/k_0 L_n$ or $4|k - k_0|c^2/L_s\omega_{pe}^2$, where L_n and L_s are the local density and temperature scale lengths.[10] For the Raman instability, the inhomogeneous threshold is $v_0^2/c^2 > 4(k - k_0)/k^2 L_n$.[5,10] For a finite-size plasma of length L, convective loss also leads to a threshold condition $L/L_1 > 1$.

The enchanced backscatter observed in laser target experiments is probably due to the Brillouin instability.[12] The fraction of light reflected is not always large, presumably due to the large size of β or to the relatively small scale length of the expanding underdense plasma.

Discussions with S. Bodner, J. DeGroot, Y. C. Lee, and C. Nielson are gratefully acknowledged.

*Work performed under the auspices of the U.S. Atomic Energy Commission.

[1a]W. L. Kruer and J. M. Dawson, Phys. Fluids 15, 446 (1972), and many references contained therein to early work in the field.

[1b]J. P. Freidberg, R. W. Mitchell, R. L. Morse, and L. I. Rudsinki, Phys. Rev. Lett. 28, 85 (1972).

[2]D. W. Forslund, J. M. Kindel, and E. L. Lindman, Phys. Rev. Lett. 29, 249 (1972); J. M. Kindel, Bull. Amer. Phys. Soc. 17, 1043 (1972); E. L. Lindman, D. W. Forslund, and J. M. Kindel, *ibid.* 17, 1044 (1972); J. M. Kindel, D. W. Forslund, and E. L. Lindman, *ibid.* 17, 1044 (1972).

[3a]L. M. Gorbunov, Zh. Eksp. Teor. Fiz. 55, 2298 (1968) [Sov. Phys. JETP 28, 1220 (1969)]; L. M. Gorbunov and V. P. Silin, Zh. Tekh. Fiz. 39, 3 (1969) [Sov. Phys. Tech. Phys. 14, 1 (1969)].

[3b]S. E. Bodner and J. L. Eddleman, Lawrence Livermore Laboratory Report No. 73378, 1971 (unpublished).

[4]M. V. Goldman and D. F. DuBois, Phys. Fluids 8, 1404 (1965); R. E. Kidder, in *Physics of High Energy Densities, Proceedings of the International School of Physics "Enrico Fermi," Course XLVIII,* edited by P. Cadirola (Academic, New York, 1971), p. 343; N. Bloembergen and Y. R. Shen, Phys. Rev. 141, 298 (1966); C. G. Comisar, Phys. Rev. 141, 200 (1966).

[5]C. S. Liu, Institute for Advanced Study, Princeton University, Report No. C003237-11, 1972 (unpublished); J. Drake, Y. C. Lee, and C. S. Liu, Bull. Amer. Phys. Soc. 17, 1065 (1972); A. G. Litvak and V. Yu. Trakhtengerts, Zh. Eksp. Teor. Fiz. 60, 1702 (1971) [Sov. Phys. JETP 33, 921 (1971)], see Eq. (33) and let $\omega_{0s} \to \omega_{pe}$.

[6]J. S. Clarke, H. N. Fisher, and R. J. Mason, Phys. Rev. Lett. 30, 89 (1973); J. Nuckolls, L. Wood, A. Thiessen, and G. Zimmerman, Nature (London) 239, 139 (1972); W. E. Utlaut and R. Cohen, Science 174, 245 (1971).

[7]N. M. Kroll, J. Appl. Phys. 36, 34 (1965), Sec. IIIB2; R. J. Briggs, *Electron-Stream Interactions with Plasmas* (Massachusetts Institute of Technology Press, Cambridge, Mass., 1964), p. 39.

[8]R. Z. Sagdeev and A. A. Galeev, *Nonlinear Plasma Theory* (Benjamin, New York, 1969), p. 16.

[9]This results in an x-type breaking [see Fig. 3(b) of Ref. 2].

[10]M. N. Rosenbluth, Phys. Rev. Lett. 29, 565 (1972).

[11]C. L. Tang, J. Appl. Phys. 37, 2945 (1966); R. V. Johnson and J. H. Marburger, Phys. Rev. A 4, 1175 (1971); Kroll, Ref. 7; R. Y. Chiao, C. H. Townes, and B. P. Stoicheff, Phys. Rev. Lett. 12, 592 (1964).

[12]R. P. Godwin and G. H. McCall, private communication; J. N. Olsen *et al.*, Bull. Amer. Phys. Soc. 17, 972 (1972); C. Yamanaka *et al.*, Institute of Plasma Physics, Nagoya University, Report No. IPPJ-117, 1972 (unpublished); J. W. Shearer *et al.*, Phys. Rev. A 6,

764 (1972); P. Belland *et al.*, Appl. Phys. Lett. 21, 32 (1972); K. Büchl *et al.*, in *Laser Interaction and Related Plasma Phenomena*, edited by H. J. Schwarz and H. Hora (Plenum, New York, 1971), p. 503; K. Eidmann and R. Sigel, Max-Planck-Institut für Plasmaphysik, Garching, Report No. IPP IV/46, 1972 (unpublished).

Josephson Effects at High Current Density*

H. A. Notarys, M. L. Yu,† and J. E. Mercereau
California Institute of Technology, Pasadena, California 91109
(Received 26 February 1973)

Effects of large phase gradients on the Josephson relation have been estimated by a modification of the Aslamazov-Larkin theory. The results are applied to explain the Dayem-Wyatt effect.

In some circumstances current density associated with the Josephson phenomena can be quite large. When this occurs, effects due to the spatial variation of the quantum phase may become important. Ordinarily, for insulating tunnel barriers, such effects are negligibly small because of the relatively low current density associated with this type of barrier. However, these effects could become significant in junctions in which the dimension parallel to the current flow approximates the de Broglie wavelength of the current. This Letter outlines an analysis of that situation based on a modification of the Aslamazov-Larkin theory.[1] The results of the analysis are used to describe the large Dayem-Wyatt effect[2] in proximity-effect bridges.[3]

In the proximity-effect bridges, the cross section is typically about 10^{-8} cm^2 and thus, for a given current, the current density is about 10^5 times that in the usual superconducting-normal-superconducting (SNS) tunnel junction.[4] Experimental results on the variation of critical current with temperature for a typical short tin-gold proximity-effect bridge are given as the solid line in Fig. 1. The current is exponential in temperature as predicted[5] for SNS junctions, but varies with temperature somewhat more rapidly than anticipated. Application of rf radiation in general enhances the critical current of these bridges. Figure 1 also shows the maximum enhanced supercurrent for this bridge when irradiated by 2-GHz radiation.

The usual Josephson analysis considers current flow through a junction region separating two superconductors of constant phase, φ_1 and φ_2. Aslamazov and Larkin (AL) showed that at low current density Josephson's result also followed from a model which treated the junction as a two-phase region in which the amplitude of the separate phases was strongly position dependent.

They assumed that in the region of a junction separating two similar superconductors 1 and 2, the wave function was composed of two terms,

$$\Psi = \psi_1 + \psi_2 = \psi_0\{f(x)\exp(i\varphi_1) + [1 - f(x)]\exp(i\varphi_2)\},$$

where $f(x)$ is a function which rapidly goes to unity in superconductor 1 and zero in superconductor 2, and ψ_0 is the undisturbed amplitude far from the junction. Thus the first part of the wave function above is phase coherent with superconductor 1 and the second part is phase coherent with superconductor 2. If current is defined in terms of the usual gradient operator, AL showed that the current resulting from this wave function

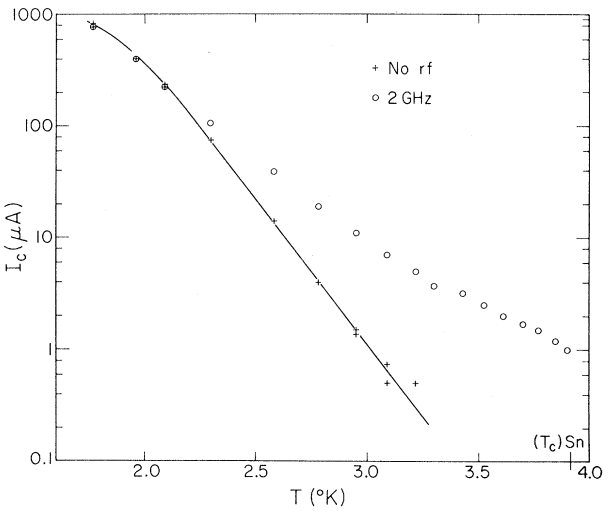

FIG. 1. Temperature dependence of the critical current of a Sn/Au proximity-effect bridge. Crosses, data points without external rf; circles, those for maximum enhancement by a 2-GHz rf field. T_c(Sn) is the transition temperature of the tin film. Bridge dimensions: length, 1 μm; width, 39 μm; thickness, 0.1 μm and resistance, 10 mΩ.